BIOLOGICAL SCIENCES: Neuroscience.

Waves of maturation and senescence in micro-structural MRI markers of human cortical myelination over the lifespan

Abbreviated title: Maturational waves of human cortical myelination

Håkon Grydeland[a], Petra E. Vértes[b], František Váša[b], Rafael Romero-Garcia[b], Kirstie Whitaker[b,c], Aaron F. Alexander-Bloch[b], Atle Bjørnerud[a,d], Ameera X. Patel[b], Donatas Sedervicius[a], Christian K. Tamnes[e], Lars T. Westlye[e], Simon R. White[f], Kristine B. Walhovd[a,d], Anders M. Fjell[a,d,1], Edward T. Bullmore[b,g,h,i, 1]

[a] Research Group for Lifespan Changes in Brain and Cognition, Department of Psychology, University of Oslo, 0317 OSLO, Norway
[b] Department of Psychiatry, University of Cambridge, Cambridge, CB2 0SZ, UK
[c] The Alan Turing Institute, London, NW1 2DB, UK
[d] Department of Physics, University of Oslo, 0371 OSLO, Norway
[e] Department of Psychology, University of Oslo, 0317 OSLO, Norway
[f] MRC Biostatistics Unit, University of Cambridge, Cambridge CB2 0SR, UK
[g] Cambridgeshire and Peterborough NHS Foundation Trust, Huntingdon, PE29 3RJ, UK
[h] MRC/Wellcome Trust Behavioural and Clinical Neuroscience Institute, University of Cambridge, Cambridge, CB2 3EB, UK
[i] Immuno-Inflammation Therapeutic Area Unit, GlaxoSmithKline R&D, Stevenage SG1 2NY, UK

[1] A.M.F and E.T.B contributed equally to this work.

Corresponding author: Håkon Grydeland, Department of Psychology, University of Oslo, PO Box 1094 Blindern, 0317 OSLO, Norway, phone: +4722845093, email: hakon.grydeland@psykologi.uio.no

Keywords: lifespan, cortical development, aging, magnetic resonance imaging, micro-structure, myelin, derivative, penalized splines, brain networks

Conflicts of Interest: The authors declare no competing financial interests. ETB is employed half-time by the University of Cambridge and half-time by GlaxoSmithKline; he holds stock in GSK.

Abstract

Seminal human brain histology work has demonstrated developmental waves of myelination. Here, using a micro-structural magnetic resonance imaging (MRI) marker sensitive to myelin, we studied fine-grained age differences to deduce waves of growth, stability, and decline of cortical myelination over the life-cycle. In 484 participants, aged 8-85 years, we fitted smooth growth curves to T1- to T2-weighted ratio in each of 360 regions from one of 7 cytoarchitectonic classes. From the first derivatives of these generally inverted-U trajectories, we defined three milestones: the age at peak growth; the age at onset of a stable plateau; and the age at the onset of decline. Age at peak growth had a bimodal distribution comprising an early (pre-pubertal) wave of primary sensory and motor cortices and a later (post-pubertal) wave of association, insular and limbic cortices. Most regions reached stability in the 30s but there was a second wave reaching stability in the 50s. Age at onset of decline was also bimodal: in some right hemisphere regions, the curve declined from the 60s, but in other left hemisphere regions, there was no significant decline from the stable plateau. Network analysis of the micro-structural connectome revealed that late developing (second wave) regions had significantly higher degree and other measures of centrality. These results are consistent with regionally heterogeneous waves of intracortical myelinogenesis and age-related demyelination, which may be relevant to the onset of neuropsychiatric disorders, and dementia, and the staged acquisition and decline of motor and cognitive skills over the course of the life-cycle.

Significance Statement

Characterizing how the human cerebral cortex normally grows to maturity and then declines across the life-span could serve as a fundamental benchmark to identify aberrant developmental trajectories thought to underlie neuropsychiatric disorders emerging in young adults, and dementia in older people. We measured a magnetic resonance imaging marker linked to myelin in nearly 500 participants, aged 8-85 years. We showed how key milestones of growth, stability, and decline occur in waves, with generally primary motor and sensory regions constituting the early wave, and association regions the late wave. Later maturing regions had more connections to other regions. Our results suggest regionally heterogeneous waves of myelinogenesis and age-related demyelination, potentially related to the onset of neuropsychiatric disorders, and dementia.

The cortex contains myelinated axons (1) critical for efficient neuronal communication (2). More than a century ago, Paul Flechsig (1847-1929) noted that cortical myelination did not occur simultaneously in all regions, but rather in a succession of waves peaking at different ages (3). Motor and sensory cortical regions myelinated earlier than association cortical regions. Yakovlev and Lecours (4) extended this notion of waves of myelinogenesis, and noted how intracortical fibres of the association cortex appeared to have long myelination cycle, demonstrating an immature "greyish pallor" beyond the third decade of life. Convergently, rodent work has shown myelin-forming oligodendrocyte cells are produced in waves (5). Specifically, three waves of oligodendroglial proliferation have been described, peaking at different stages of forebrain development before and after birth (6). Later in life, primate histology studies have reported cortical myelin degeneration, and aberrant remyelination (7).

Magnetic resonance imaging (MRI) has allowed for the indirect study of myelin using volume and other measures likely related to myelin in development (8), adulthood, and aging (9). Such studies, focusing mainly on the white matter (WM) of the cerebrum, seem to largely support Flechsig's idea of myelination heterochronicity (10). van der Knaap and Valk (11) studied myelination during the first postnatal year using T1- and T2-weighted images, delineating 5 stages, or waves, of myelination. However, there have been no attempts to test Flechsig's notion of cortical waves during childhood and adolescence, and whether similar patterns could be found late in life.

There have been only a few studies encompassing a sufficient age range to investigate myelinogenesis, from childhood to old age, comprehensively across the human cortex. Studying the WM, Kochunov*, et al.* (12) fitted linear models to diffusion tensor imaging data before and after the age at peak fractional anisotropy (a marker of WM tract organization) in participants aged 11-90 years. In nine WM tracts, they reported that tracts with a faster rate of maturation had a faster rate of age-related decline. Yeatman, Wandell and Mezer (13) fitted a piecewise linear model of R1 (a quantitative marker sensitive to myelin) in 24 WM pathways for participants aged 7-85 years. They found no systematic relationship between the age at which a tract matures and the age at which it begins to decline. Studying cortical myelination,

Deoni *et al.* (14) found logarithmic increases in myelin water volume fraction (a quantitative measure sensitive to myelin) with age in children aged 1 to 6 years. Using methods sensitive to myelin based on magnetization transfer, Whitaker*, et al.* (15) showed a linear cortical myelin increase for participants aged 14-24 years. Callaghan*, et al.* (16) reported stable levels of myelin until around 60 years of age, followed by decrease, in several cortical regions including the Heschl's gyri, for participants aged 19-75 years.

Moreover, the lifespan studies (12, 13) yielded mixed support for the concept that decline occurs in reverse order to growth of myelination. This so-called "last in, first out" hypothesis (17) suggests that regions that myelinate last in the course of development, are the first to demyelinate later in life, i.e. are more affected by age. This heterochronic pattern has been related to association cortices compared with sensory cortices (17), possibly due to their underlying cytoarchitecture. The association cortex is particularly well connected, specialised for multimodal integration, and underpins most complex behaviours (18). Therefore, these regions might need to remain plastic for as long as possible to refine their connections (19) and consolidate them by a prolonged phase of myelination. In line with this reasoning, but in contrast to the "last in, first out" hypothesis, these regions could be the last to decline ("last in, last out"). The high connectivity of the association cortex also raises the question of how patterns of myelination relate to how the brain is organised as a network. Particularly, whether the most well-connected "hub" regions are later to mature and to decline (15).

In this context, we aimed to investigate myelination across the cortex in humans (N=484, aged 8-85 years), using a micro-structural MRI marker sensitive to myelination (20): the ratio of T1- and T2-weighted MRI images (T1w/T2w). Variation in T1w/T2w has been shown to match histologically-derived myelin content (21), and has been related to individual differences in electrophysiology (22), and cognition (23). T1w/T2w has shown positive relationships with age in development and early adulthood, and negative relationships with age in later life (23, 24). Here, we move further by testing Flechsig's theory of waves across the life-span. From the T1w/T2w maps, we fitted smooth age-trajectories for 360 cortical regions (20) in each of 7 cytoarchitectonic classes (25). The first derivatives of these cross-sectionally

estimated cortical growth curves allowed us to define three key micro-structural milestones, namely age at peak growth, age at onset of stability, and age at onset of decline. We analysed the distribution of these milestones for deviations from unimodality (i.e. at least bimodality). We related the timing of the milestones both to (i) the estimated maximum rates of maturation and decline in each region; and (ii) the topological properties of each node in the structural covariance network estimated on average across a subset of participants.

On this basis, we tested three hypotheses: i) the timing of micro-structural milestones – age at peak growth, age at onset of stability, and age at onset of decline - has at least a bimodal distribution indicative of successive waves of change in myelination, ii) timing of these milestones is related to rates of micro-structural maturation and decline, and iii) the variation in milestones and rates of micro-structural growth and decline relate to cytoarchitectonic properties, and network topology, namely connectivity strength or hubness of regions in the anatomical network. We particularly expected the association cortex to develop and decline differently compared with the most heavily myelinated primary motor and sensory cortices.

Results

Trajectory and milestones of age-related change in micro-structural MRI. The average T1w/T2w ratio map across all participants shows that more highly myelinated primary motor and sensory areas have higher T1w/T2w values compared with association areas (**Fig. 1A**). The global trajectory of T1w/T2w, on average over all cortical regions in each participant, is approximately an inverted-U function of age over nearly 80 years of the lifespan (**Fig. 1B**). There is a maturational increase or growth of T1w/T2w in the first part of life, before the curve gradually levels off and a plateau is reached in middle age, followed by a later period of decline from around 60-65 years.

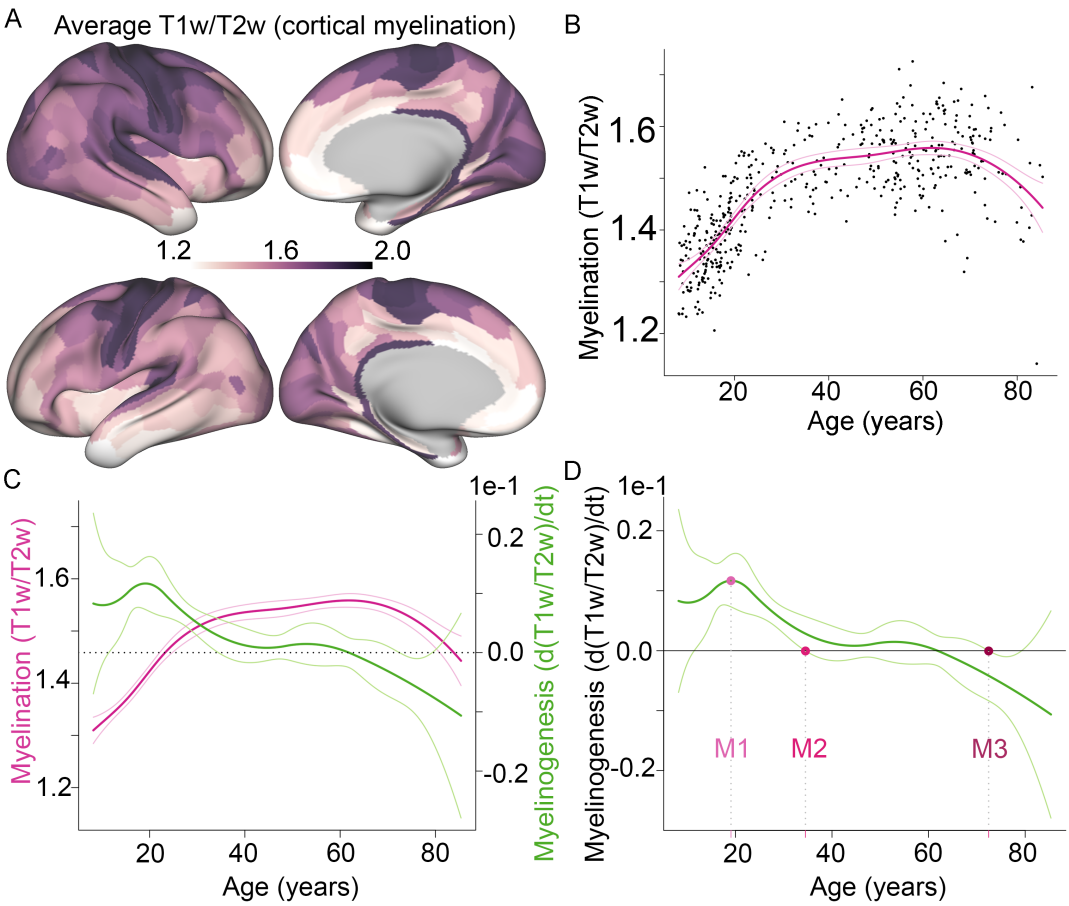

Fig. 1. Milestones of human intra-cortical myelinogenesis estimated from non-linear growth curves of T1w/T2w MRI data measured across the life-cycle. A. Surface maps of T1w/T2w values averaged across the nearly 80 years of the lifespan (N=484). **B**. Average T1w/T2w values across the 360 regions for each participant plotted against the participants' age. The fitted cubic spline and the 99% CI are plotted in magenta. **C.** The fitted cubic spline and the 99% CI (magenta) from **B**, and the estimated rate of change (first derivative) and the 99% CI (green). **D.** The 3 milestones: M1 = peak growth age (19 years), M2 = onset stability age (37 years), M3 = onset decline age (69 years).

To quantify this age-related micro-structural variation more precisely, we estimated the slope of the T1w/T2w curve at each point in time, t, i.e., the first derivative of the trajectory, d(T1w/T2w)/dt (**Fig. 1C**). We then estimated 99% confidence intervals (CIs) for both the curve and its first derivative, which we used to rigorously define three key milestones (M1, M2, M3). M1, peak growth age, was defined as the age of

maximum positive rate of change in T1w/T2w; M2, onset stability age, was defined as the earliest age after M1 at which the 99% interval for the derivative curve included zero, indicating that there was no significant growth or decline in T1w/T2w; and M3, onset decline age, was defined as the earliest age after M2 at which the 99% interval for the derivative curve did not include zero, indicating that there was significant negative rate of change in T1w/T2w (**Fig. 1D**). For the whole brain trajectory, peak growth age (M1) occurred at 19 years, onset stability age (M2) at 34 years, and onset decline age (M3) at 72 years. From the derivative curves we also estimated two additional metrics of interest (***SI Appendix, Fig. S1***): the maximum rate of growth in T1w/T2w (i.e. the derivative at M1), and the maximum rate of decline (i.e. the derivative at mid-point between M3 and the end of the age range).

Cortical mapping of milestones of age-related change in MRI micro-structure. We estimated all three milestones for each of 360 cortical regions and plotted the age at each milestone for each region as cortical surface maps. Peak growth age (**Fig. 2Ai,** and ***SI Appendix, Fig. S2***) occurred earlier, i.e., before 13 years of age, predominantly in areas with high myelin content such as the primary motor and sensory areas, as well as the retrosplenial cortex and right area lateral occipital 2 (please see (20) for explanation of the nomenclature), and area MT. Regions with a later peak growth age, i.e., after 13 years of age, were found in prefrontal, parietal, and temporal cortices, particularly in the right hemisphere, as well as medial occipital cortex.

Onset of stability was reached between 29 and 50 years (**Fig. 2Aii**) and was found to occur later particularly in lateral temporal, medial prefrontal and anterior cingulate cortex bilaterally, as well as in left lateral frontal cortex, with regions in general reaching a plateau later in the left hemisphere.

Onset of significant decline started between 58 and 77 years of age (**Fig. 2Aiii**) in 170 regions, while 190 regions, particularly in the left hemisphere, did not show a significant decline. In both hemispheres, onset of decline was observed earlier in motor and sensory cortices, and the retrosplenial complex.

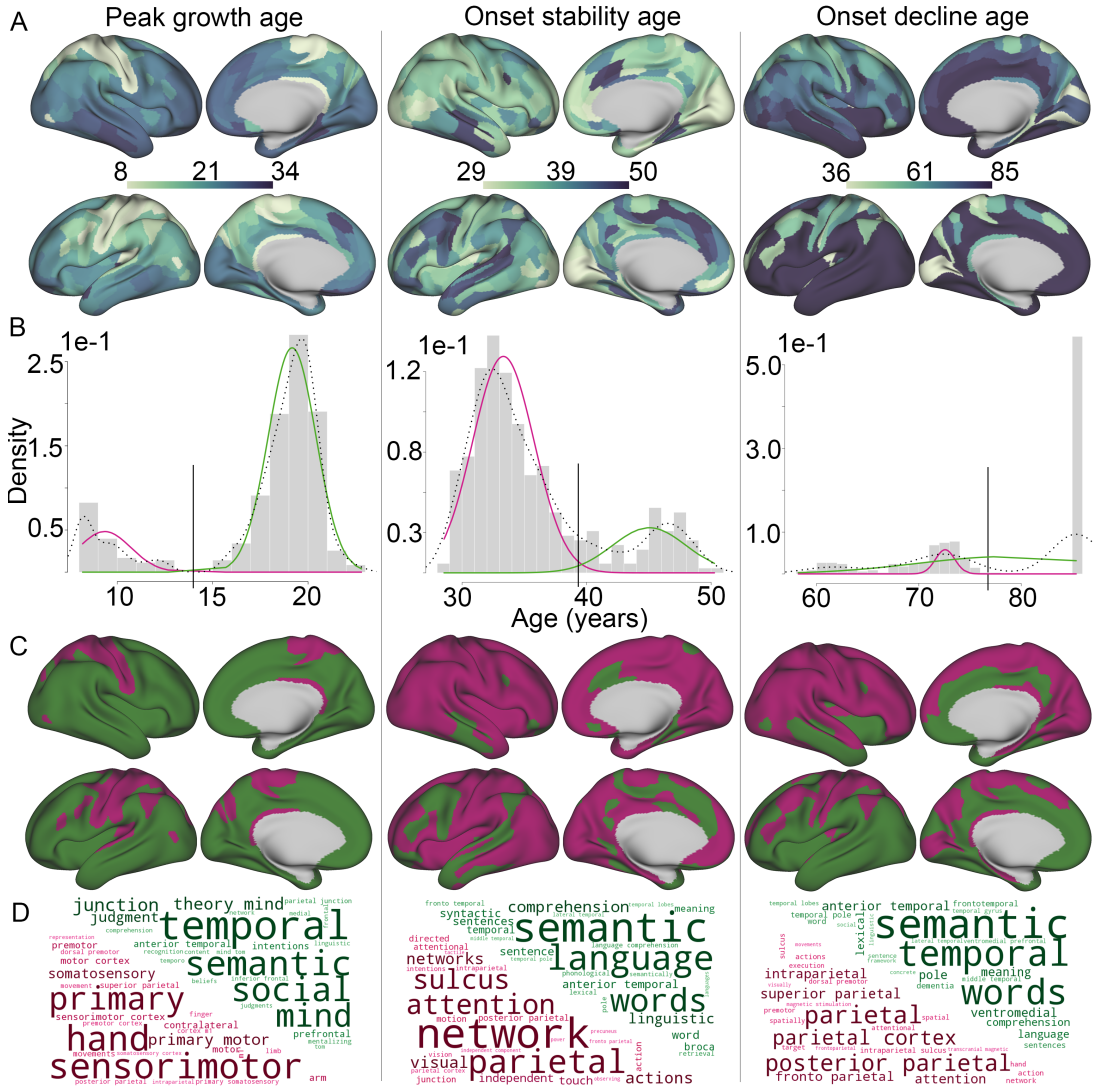

Fig. 2. Intracortical T1w/T2w MRI milestone maps, and bimodal distributions suggesting that timing of generation and degeneration of myelination occurs in waves. A. Surface maps of peak growth age, onset stability age, and onset decline age. **B**. Histograms for i) peak growth age, ii) onset stability age, and iii) onset decline age with the fit of a 2-component Gaussian mixture model overlaid (in magenta and green). Age used for dichotomisation into early and late waves (grey vertical bar) for peak growth age was 12.7 years, stability 39.5 years, and decline 77 years. Black dotted line = probability density. **C**. Surface maps of early (magenta) and late (dark green) waves based on **B**. **D**. Word clouds based on correlations with NeuroSynth meta-analysis maps for the early and late waves at each milestone.

Bimodal distributions of micro-structural milestones. Inspection of the distributions of each of the milestones provides intuitive support for the existence of waves of change in T1w/T2w. For each milestone, there are two distinct peaks (**Fig. 2B)**, suggesting that the distribution is not unimodal but at least bimodal (see also quantile-quantile plots, ***SI Appendix, Fig. S3***). We tested this observation formally, finding evidence for significant non-unimodality in all milestone distributions (Hartigan's dip test, $P < 0.001$). A two-component mixture of Gaussian distributions was fitted to each of the milestone distributions, providing a significantly better fit than a unimodal model in all cases (bootstrap likelihood ratio test, all $P < 0.001$). Each milestone distribution could thus be partitioned into an early wave and a late wave (**Fig. 2B)**, and each cortical region could be assigned to the early or late waves of each milestone (**Fig. 2C**).

The first wave of peak growth occurred at a mean age of 9.4 years ([95% CI [9.0, 9.7]) in relatively few areas of primary cortex, specialised for motor and somatosensory function; the second wave occurred at a mean age of 19.5 years (95% CI [19.2-19.7]) in a larger number of association areas, specialised for semantic and social functions, such as theory of mind (determined through a search of neurosynth.org (26), **Fig. 2D**).

The first wave of onset of stability occurred at a mean age of 33.3 years (95% CI [33.0, 33.6]), and involved areas of parietal cortex specialised for attention. A smaller number of areas, mostly located in the left hemisphere and specialised for semantic language functions, reached stability later with mean age of onset 45.1 years (95% CI [44.4, 45.8]).

The first wave of onset of decline occurred at a mean age of 68.8 years (95% CI [67.8, 69.8]), and involved mainly right hemisphere frontal and parietal regions specialised for attention and executive functions. The second wave in this case represented a large number of regions, mainly in the left hemisphere and specialised for semantic language functions, which did not show evidence of significant decline within the age range of the sample (up to 85.4 years).

Rates of maturation and decline of cortical micro-structure. Surface maps of the regional variation in rate of maturation, and the rate of decline are shown in **Fig. 3A** and ***SI Appendix, Fig. S4***. We observed higher rates of maturation and decline in highly myelinated areas of primary motor and sensory areas and lower rates of maturation and decline in lightly myelinated frontal and temporal cortical areas. The average T1w/T2w map (**Fig. 1A**) and the rate of peak growth map (**Fig. 3Ai**) were strongly positively correlated (Spearman's $\rho = 0.75$, $P < 0.001$). Conversely, the average T1w/T2w map was strongly negatively correlated with the rate of decline map (**Fig. 3Aii**; Spearman's $\rho = -0.67$, $P < 0.001$). As expected given these results, the regions with high rates of maturation also had high rates of decline (**Fig. 3B**; Spearman's $\rho = -0.59$, $P < 0.0001$), i.e. a "fastest in, fastest out" pattern.

These maturation and decay rates of T1w/T2w, respectively indicative of rates of cortical myelination and demyelination, were significantly different between waves of myelinogenesis as defined by the three milestones, M1-M3 (**Fig. 3C**). The rate of maturation was significantly more positive, and the rate of decline was significantly more negative, in the first M1 wave of regions that reached peak growth before puberty than in the second M1 wave of regions that reached peak growth after puberty (***SI Appendix, Table S1***). Likewise, the first M2 wave of regions, which reached onset of stability earlier, had more positive rates of maturation than the second M2 wave of regions, which reached stability later. Finally, a similar pattern was evident for the M3 milestone: regions in the first wave, which reached onset of decline earlier, had more positive rates of maturation. Regions in the second M3 wave had less positive rates of maturation and less negative rates of decline (close to zero).

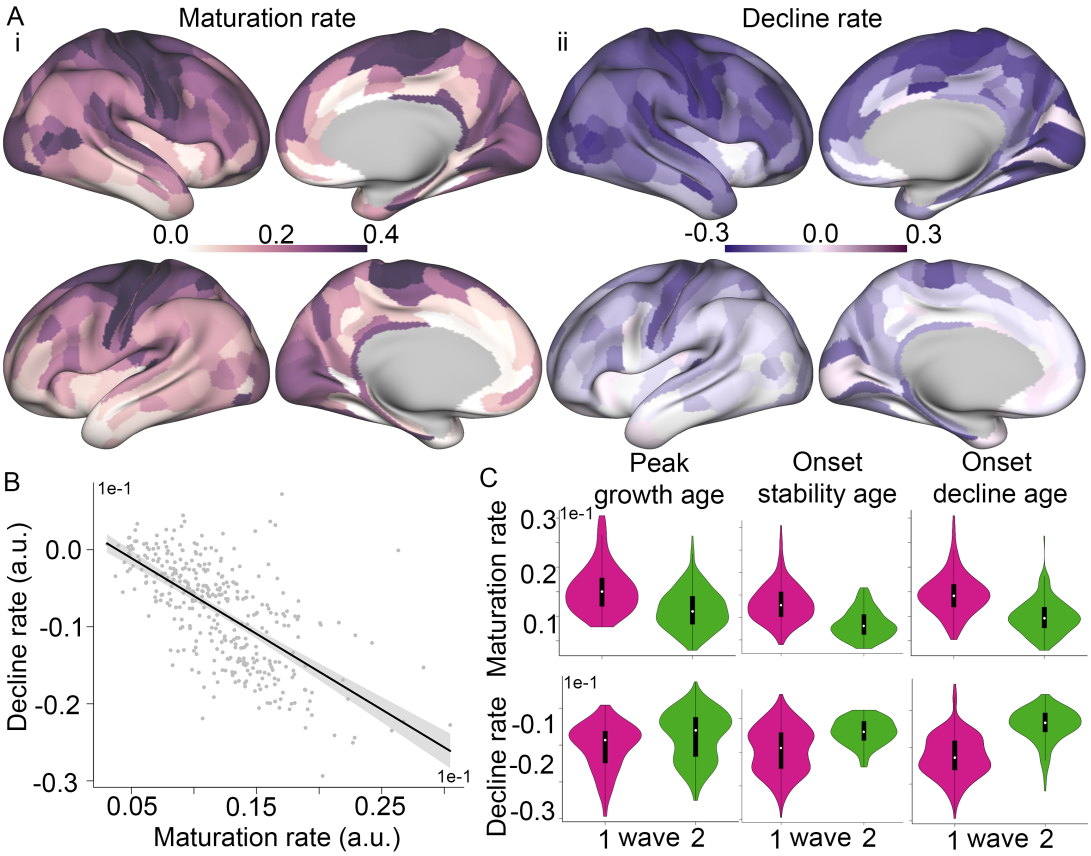

Fig. 3. Milestones of intracortical MRI growth curves were related to rates of change in generation and degeneration of myelination. **A**. Surface maps depicting rates of i) peak growth (i.e. the derivative at M1), and ii) decline (i.e. the derivative at mid-point between M3 and the end of the age range). **B**. Inter-regional association between micro-structural maturation, and decline rate. Regression line in black (R^2 = 0.43, $p < 0.001$), the 95% CI in shaded grey. **C**. Violin plots of the relationship between rate of peak growth (top row), and decline (bottom row) with age of peak maturation (first column), stability, decline, respectively, showing significant differences between early (magenta) and later (green) waves at each milestone.

Cytoarchitectonics. We tested the relationship between cortical histology and milestones of the T1w/T2w trajectory by classifying the 360 regions according to its membership of one of 7 cytoarchitectonic classes defined by the von Economo and Koskinas atlas (25) (***SI Appendix, Fig. S5A***). Different cytoarchitectonic classes and cerebral hemispheres were differently represented in the two waves at the M1 milestone (***SI Appendix, Fig. S5*B**). The proportion of regions reaching peak growth

before puberty was significantly different between cytoarchitectonic classes, with a higher proportion of primary motor and primary sensory cortices in the first wave than in the second wave (χ^2= 65, df=6, P_{FDR} = 1× 10^{-10}). The differences in proportion of cytoarchitectonic classes in the first and second waves of the M2 milestone were not significant after multiple comparison correction (χ^2= 14, df=6, P_{FDR} = 0.126, $P_{uncorrected}$ = 0.035). However, there were significant differences between the first and second waves of the M3 milestone, with a higher proportion of association cortical areas, especially in the left hemisphere, represented in the second wave (χ^2= 37, df=6, P_{FDR} = 1.3 × 10^{-5}).

Connectomics. To investigate how the local cortical milestones of age-related change in T1w/T2w might relate to the topology of the cortical connectome, we estimated the pair-wise correlation of T1w/T2w between each possible pair of regions across participants between the ages of stability and decline onset in the global curve (see **Fig. 1B**; 37 and 69 years, respectively), that is, a period with relative stable T1w/T2w levels. From this micro-structural network model (***SI Appendix, Fig. S6A***), we constructed a binary graph by retaining the 10% strongest connections which could be decomposed into a community structure of modules (***SI Appendix, Fig. S6B***). For each regional node, we then estimated its degree centrality (27), i.e., the number of edges connecting it to the rest of the network; its intra-modular degree, i.e., the number of edges connecting it with nodes in the same module; and its inter-modular degree, i.e., the number of edges connecting it with nodes in other modules. The network had a fat-tailed degree distribution (**SI Appendix, Fig. S6C**), indicative of so-called hub regions. These high degree regional nodes were mainly found in frontal, parietal, and temporal association cortices (**Fig. 4Ai-ii**).

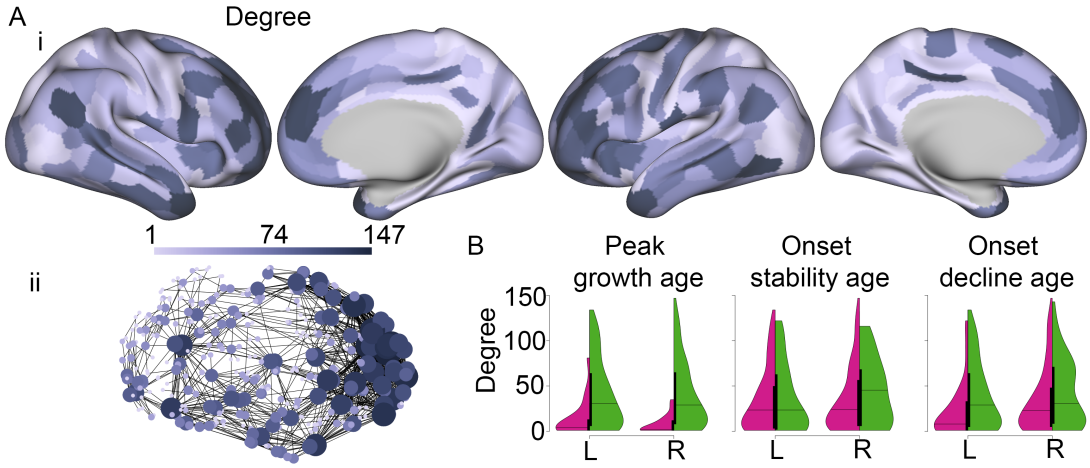

Fig. 4. Hubs of the structural covariance connectome have a long period of adolescent and early adult myelination, with delayed onset of maturity, but later onset of decline. A. The structural covariance network. High-degree centrality hubs were concentrated anatomically in association cortical areas. i. Surface maps of degree. ii. Network representation, nodes are coloured and sized by degree (only the top 2% strongest connections are shown for clarity). **B**. Violin plots, split per hemisphere and early (magenta) and late (green) waves, for peak growth age, onset stability age, and onset decline age. L/R = left/right hemisphere.

There were significant differences in nodal topology between the two waves of the M1 milestone (**Fig. 4B**, and ***SI Appendix, Fig. S7*** and ***Table S1***). Regions which reached peak growth before puberty had significantly reduced total degree, intra-modular degree, and inter-modular degree, compared to regions which reached peak growth after puberty. Likewise, there were significant differences in nodal topology between the two waves of the M3 milestone. Regions in the second wave, which did not show onset of significant decline, had significantly higher total degree, and inter-modular degree, than regions in the first wave which had onset of decline in the 60s. There were no significant differences in nodal topology between regions in the first and second waves of the M2 milestone.

Discussion

Based on a cross-sectional sample covering nearly 8 decades of the lifespan, we delineated the age-related trajectory of maturation and senescence of a micro-

structural MRI marker linked to myelin. We found indications of maturation and decay occurring in stages, or waves, at three key milestones: age at peak growth, age at onset of stability, and age at onset of decline. Importantly, we also observed that regions in the first wave of developmental milestones had faster rates of maturation and faster rates of decline. This result contradicted the "last in, first out" hypothesis (17), according to which early maturing regions should be more protected from age-related decline than late maturing regions. We found the opposite. By linking the timing of milestones to the cytoarchitectonic atlas of von Economo and Koskinas, we found that early maturing regions were histologically classified mainly as heavily myelinated primary motor and sensory cortices, whereas later maturing regions were mainly association, limbic and insular cortices. We also found that the high degree hubs of the anatomical connectome had significantly later age at peak growth and later age at onset of decline than less well-connected nodes in the structural covariance network.

Waves of myelinogenesis as implicated by age differences in milestones. We observed a bimodal distribution of all milestones. In accordance with histological results based mostly on early childhood brains (3, 4), we interpret this finding as suggestive of waves of myelinogenesis. This concept has not been studied within a lifespan perspective, and the observations could be conceptualized as "echoes" in later life of earlier waves of neuro- and glio-genesis (28). Another interesting hypothesis relates post-pubertal myelination to sexual maturity (29), and the changes in executive and social cognition associated with adolescence (30). This suggestion relates to the timing of peak myelination which occurred in one wave before and one wave after puberty. The post-pubertal wave regions were more concentrated in association, insular, and limbic cortices, and this accords with the suggested link between post-pubertal myelination and the onset of psychiatric diseases during adolescence and early adulthood (31, 32).

The "last in, first out" hypothesis. The present micro-structural results indicated a "last in, last out" pattern, which is in contrast to the "last in, first out" hypothesis (17). MRI lifespan studies using grey matter (GM) macro-structural measures have found support for this hypothesis (e.g. Douaud*, et al.* (33)), while others using micro-structural measures of the cortex (e.g. Westlye*, et al.* (34)) have not. One possible

explanation for this discrepancy between the lifespan trajectories for macro- versus micro-structural aspects of the cortex may be that loss of myelin in primary motor and sensory areas could offset cortical thinning. As both the cortex and the subjacent white matter become "greyer" due to demyelination, the WM/GM boundary recedes, making thinning appear less extensive (35). This process is essentially an inversion of the suggested explanation of thinning in childhood and adolescence, where increased myelination makes the deeper layers of cortex appear "whiter" (36). The more negative macro-structural age-relationships observed in the lightly myelinated late wave areas might be driven more by processes other than demyelination, for instance reduction in dendritic spine density of pyramidal neurons (37). Another possibility is that demyelination with age is offset by other types of myelin degeneration, such as the formation of redundant myelin and increasing thickness of myelin sheaths reported in older aged monkeys (7).

The gain-predicts-loss hypothesis. Although we did not find a clear relationship between age at onset of stability and age at onset of decline, we did find that regions showing higher rates of peak growth, and doing so relatively early, also showed an early onset of decline and a faster rate of decline. The mainly primary motor and sensory regions showed earlier and faster rates of cortical myelination and earlier and faster rates of cortical demyelination with high age. Thus, in addition to a "last in, last out" pattern, our results fit partly with a "gain-predicts-loss" hypothesis (13). This hypothesis predicts that the rate of change in development will be mirrored by the rate of decline in aging. We found that the aging process is not exactly the reverse of development, in contrast to R1 trajectories of WM tracts (13). Instead, the T1w/T2w trajectories increased more steeply in development compared with less rapid rates of decline later in life, as in the diffusivity trajectories of the same tracts (13). Interestingly, the differences in rate of development and decline in primary motor and sensory regions compared with association, limbic and insular regions, fits well with the processing-speed theory of adult age differences in cognition (38). This theory proposes that processing speed reduction leads to the age-related decline in higher-order cognition, such as memory and reasoning. In development, a similar idea, but in an opposite direction with increased speed, has been proposed (39). Accordingly in this context, processing speed relates more strongly to sensorimotor areas than

association cortices, while association cortices relate more strongly to higher-order cognitive functioning (40).

Connectomics. Another feature of our findings was the relationship between waves of (de-)myelination and high degree network regions of the anatomical connectome, so-called hubs. We found that hubs had significantly later age at peak growth and later age at onset of decline than less well-connected nodes in the structural covariance network. Flechsig (3) observed that association regions were the focus of a relatively late wave of myelinogenesis. In our data and previous studies (15, 41), hub regions are disproportionately located in association cortex. Thus, the observation of different micro-structural trajectories for hubs compared with primary motor and sensory areas aligns with Flechsig's idea. Here, we extend this notion by showing that hub regions seem to be the focus of a relatively late wave of myelinogenesis also later in life. Although the relationships were not strong, the result followed from our earlier findings that association cortices (and limbic and insular cortices) show later and lower rates of micro-structural maturation and decline compared with motor and sensory cortex. As discussed in (15), cortical myelination in development might be topologically targeted to optimize hub performance. Similar processes might be at play in aging, which might break down in disorders such as Alzheimer's disease (42).

Methodological issues. The results are based on cross-sectional analyses, and longitudinal data are needed to estimate measures of individual change. The T1w/T2w ratio measure used here stems from T1- and T2-weighted scans, at a conventional resolution. Using a quantitative measure at high resolution (43) likely would have been preferable for sensitivity and specificity. Many regions (particularly in the left hemisphere) did not exhibit age-related decline, which contrasts with other MRI markers such as cortical thickness. Hemispheric asymmetry in patterns of age-related cortical volume shrinkage in aging have been inconsistent (44). Still, verbal abilities are relatively well preserved in aging (45), and a potential relationship between intracortical micro-structure and preservation of verbal abilities, which are known to depend mainly on the left hemisphere (46), constitutes an interesting hypothesis for future research.

Summary. Peak growth, stability, and decline of an MRI measure related to intracortical myelination proceeds in stages, or waves, in different regions. Primary motor and sensory regions reached all milestones earlier than association, limbic, and insular regions. The results contrasted with the so-called "last in, first out" hypothesis. Instead, the findings suggested a "last in, last out" pattern, where the regions less likely to show decline in aging were slowly maturing, association cortical hubs. In addition, the results fit partly with a gain-predicts-loss hypothesis, where regions which mature fastest, decline fastest. Future studies might benefit from looking more closely into how timing of waves relate to the onset of neuropsychiatric disorders, as well as the changes in cognitive and social skills, in development and aging.

Materials and Methods

Sample*.* Participants were included after screening for conditions assumed to affect CNS function (for details regarding *Methods*, see **SI Appendix)**. Based on the existence of a T1w and a T2w scan for each individual, and after quality control excluding a total of 18 participants due movement artefacts or overfolding in T1w, T2w, or both, we included 484 participants: 263 females (54.3%), mean age (SD) = 38.3 (22.5) years, median age= 34.6 years, age range = 8.2-85.4 years.

MRI Data Acquisition and Analysis*.* Scans were acquired using a 12-channel head coil on a 1.5-T Siemens Avanto scanner (Siemens Medical Solutions, Erlangen, Germany) at Oslo University Hospital Rikshospitalet, in one session per participant, using a 3D T1w magnetization-prepared rapid gradient echo (T1w), and a 3D T2w sampling perfection with application optimized contrasts using different flip angle evolutions sequence (T2w). T1w/T2w maps were created using the Human Connectome Project (HCP) processing pipeline (https://github.com/Washington-University/Pipelines), including processing with the Freesurfer 5.3 suite (http://surfer.nmr.mgh.harvard.edu). The T1w volume was divided on the aligned (using *bbregister* (47) and spline interpolation (21)) T2w volume, creating a T1w/T2w ratio volume. To estimate regional T1w/T2w, we used a multi-modal parcellation to divided each cerebral hemisphere into 180 areas (20). We sampled T1w/T2w values from the WM/GM boundary, at 9 intermediate cortical depths (10% intervals), and at the GM/CSF boundary (***SI Appendix, Fig. S8***). Here we focused on T1w/T2w

measures at 70% depth from the pial surface to avoid partial volume effects (43) (***SI Appendix, Fig. S9***).

Estimations of Growth Curve Trajectories*.* To fit age trajectories without assuming a specific shape of the relationship *a priori*, we used penalized splines (48, 49). Eight piecewise cubic B-spline basis functions were used to fit a smooth, non-linear curve from the weighted sum of these functions (***SI Appendix, Fig.* S10**). We calculated the derivative, i.e. the slope at each point along the curve, as the differences (Δy) between the predicted curve (using the *predict* function in R (www.r-project.org/)) from i) one set of age values, and ii) another set with slightly increased age values, divided by this increment (Δx): $\frac{\Delta y}{\Delta x}$ or $\frac{dy}{dx}$. To find significant increases or decreases, we estimated the 99% CI of the derivative. Based on this CI, we extracted 3 curve features, or milestones, namely age at peak growth, age at onset of stability, and age at onset of decline. We also estimated cross-sectional measures of the rate of growth, and the rate of decline (***SI Appendix, Fig. S1***).

Comparison with the Cytoarchitectonic Map of von Economo and Koskinas. We explored the relationship between cortical histology and the key milestones (50). Based on previous work (25, 51), we assigned each of the 360 regions to 1 of 5 cytoarchitectonic types classified according to the scheme of von Economo and Koskinas (52), reflecting the 5 structural types of isocortex, or to two additional subtypes (50): limbic cortex, and the insular cortex.

Structural Network Analyses*.* We created a structural network by employing a covariance approach (41). The community structure was obtained using the Louvain algorithm (53), and consensus clustering (54). We empirically defined the resolution parameter for modular decomposition by finding a local minimum for nodal versatility of modular affiliation (55)

Statistical Analyses. We tested for unimodality using Hartigans' dip test statistic (56). We used an expectation–maximization (EM) algorithm to fit Gaussian finite mixture models with 1 and 2 components, where a maximum of 2 components would provide proof of concept, and not be liable to over-fitting, and tested for best fit using

a bootstrap likelihood ratio test with 10000 bootstraps. To facilitate the fitting process, 9 values above 25 years of age, and 4 values around 40 years were removed from M1 and M3, respectively, before estimation and plotting. Relationships between the regional measures were tested using Spearman's rank correlation, except between rate of maturation and decline, where a linear regression was performed. To assess differences in rates of maturation and decline, respectively, between early and late waves across the 3 milestones, we calculated 99% CIs. In the cases where the CI overlapped, we tested for differences between waves by Wilcoxon rank sum test. The same approach was used to test for differences in the degree measures between waves. To test for the differences across cytoarchitectonic classes, we employed Kruskal-Wallis tests by rank, and accounted for the multiple tests performed by applying false discovery rate (FDR) correction (57).

Acknowledgements

This work was supported by the Department of Psychology, University of Oslo (to K.B.W., A.M.F.), the Norwegian Research Council (to K.B.W., A.M.F.) and the project has received funding from the European Research Council's Starting/ Consolidator Grant schemes under grant agreements 283634, 725025 (to A.M.F.) and 313440 (to K.B.W.)

P.E.V. was supported by the Medical Research Council grant number MR/K020706/1 and is a Fellow of MQ: Transforming Mental Health, grant number MQF17_24.

K.W. is supported by a research fellowship at the Alan Turing Institute under the EPSRC grant EP/N510129/1.

S.R. White was supported by the Medical Research Council, UK (Unit Programme number U105292687).

This work was supported by the NIHR Cambridge Biomedical Research Centre.

References

1. Gennari F (1782) De peculiari structura cerebri nonnullisque ejus morbis ... Paucae aliae anatom. observat. accedunt. (Ex regio typographeo, Parma).
2. Zalc B & Colman DR (2000) Origins of vertebrate success. *Science* 288(5464):271-272.
3. Flechsig P (1901) Developmental (myelogenetic) localisation of the cerebral cortex in the human subject. *The Lancet* 158(4077):1027-1030.
4. Yakovlev PI & Lecours A-R (1967) The myelogenic cycles of regional maturation of the brain. *Regional Development of the Brain in Early Life*, ed Minkowski A (Blackwell Scientific Publications, Oxford and Edinburg), pp 3-70.
5. Kessaris N, *et al.* (2006) Competing waves of oligodendrocytes in the forebrain and postnatal elimination of an embryonic lineage. *Nat Neurosci* 9(2):173-179.
6. Rowitch DH & Kriegstein AR (2010) Developmental genetics of vertebrate glial-cell specification. *Nature* 468(7321):214-222.
7. Peters A (2009) The effects of normal aging on myelinated nerve fibers in monkey central nervous system. *Front Neuroanat* 3:11.
8. Paus T, *et al.* (1999) Structural maturation of neural pathways in children and adolescents: in vivo study. *Science* 283(5409):1908-1911.
9. Bartzokis G, *et al.* (2001) Age-related changes in frontal and temporal lobe volumes in men: a magnetic resonance imaging study. *Archives of general psychiatry* 58(5):461-465.
10. Gao W, *et al.* (2009) Temporal and spatial development of axonal maturation and myelination of white matter in the developing brain. *AJNR Am J Neuroradiol* 30(2):290-296.
11. van der Knaap MS & Valk J (1990) MR imaging of the various stages of normal myelination during the first year of life. *Neuroradiology* 31(6):459-470.
12. Kochunov P, *et al.* (2012) Fractional anisotropy of water diffusion in cerebral white matter across the lifespan. *Neurobiol Aging* 33(1):9-20.
13. Yeatman JD, Wandell BA, & Mezer AA (2014) Lifespan maturation and degeneration of human brain white matter. *Nat Commun* 5:4932.
14. Deoni SC, Dean DC, 3rd, Remer J, Dirks H, & O'Muircheartaigh J (2015) Cortical maturation and myelination in healthy toddlers and young children. *Neuroimage* 115:147-161.
15. Whitaker KJ, *et al.* (2016) Adolescence is associated with genomically patterned consolidation of the hubs of the human brain connectome. *Proc Natl Acad Sci U S A* 113(32):9105-9110.
16. Callaghan MF, *et al.* (2014) Widespread age-related differences in the human brain microstructure revealed by quantitative magnetic resonance imaging. *Neurobiol Aging* 35(8):1862-1872.
17. Raz N (1999) Aging of the brain and its impact on cognitive performance: Integration of structural and functional findings. *The handbook of aging and cognition*, (Lawrence Erlbaum, Mahwah, N.J), 2nd Ed.
18. van den Heuvel MP & Sporns O (2013) Network hubs in the human brain. *Trends Cogn Sci* 17(12):683-696.
19. Glasser MF, Goyal MS, Preuss TM, Raichle ME, & Van Essen DC (2014) Trends and properties of human cerebral cortex: correlations with cortical myelin content. *Neuroimage* 93 Pt 2:165-175.

20. Glasser MF, *et al.* (2016) A multi-modal parcellation of human cerebral cortex. *Nature* 536(7615):171-178.
21. Glasser MF & Van Essen DC (2011) Mapping human cortical areas in vivo based on myelin content as revealed by T1- and T2-weighted MRI. *J Neurosci* 31(32):11597-11616.
22. Grydeland H, Westlye LT, Walhovd KB, & Fjell AM (2015) Intracortical Posterior Cingulate Myelin Content Relates to Error Processing: Results from T1- and T2-Weighted MRI Myelin Mapping and Electrophysiology in Healthy Adults. *Cereb Cortex*.
23. Grydeland H, Walhovd KB, Tamnes CK, Westlye LT, & Fjell AM (2013) Intracortical myelin links with performance variability across the human lifespan: results from T1- and T2-weighted MRI myelin mapping and diffusion tensor imaging. *J Neurosci* 33(47):18618-18630.
24. Shafee R, Buckner RL, & Fischl B (2015) Gray matter myelination of 1555 human brains using partial volume corrected MRI images. *Neuroimage* 105:473-485.
25. Scholtens LH, de Reus MA, de Lange SC, Schmidt R, & van den Heuvel MP (2016) An MRI Von Economo - Koskinas atlas. *Neuroimage*.
26. Yarkoni T, Poldrack RA, Nichols TE, Van Essen DC, & Wager TD (2011) Large-scale automated synthesis of human functional neuroimaging data. *Nat Methods* 8(8):665-670.
27. Bullmore E & Sporns O (2009) Complex brain networks: graph theoretical analysis of structural and functional systems. *Nat Rev Neurosci* 10(3):186-198.
28. Rakic P (2002) Neurogenesis in adult primate neocortex: an evaluation of the evidence. *Nat Rev Neurosci* 3(1):65-71.
29. Miller DJ, *et al.* (2012) Prolonged myelination in human neocortical evolution. *Proc Natl Acad Sci U S A* 109(41):16480-16485.
30. Blakemore SJ & Choudhury S (2006) Development of the adolescent brain: implications for executive function and social cognition. *J Child Psychol Psychiatry* 47(3-4):296-312.
31. Bartzokis G (2002) Schizophrenia: breakdown in the well-regulated lifelong process of brain development and maturation. *Neuropsychopharmacology* 27(4):672-683.
32. Paus T, Keshavan M, & Giedd JN (2008) Why do many psychiatric disorders emerge during adolescence? *Nat Rev Neurosci* 9(12):947-957.
33. Douaud G, *et al.* (2014) A common brain network links development, aging, and vulnerability to disease. *Proc Natl Acad Sci U S A* 111(49):17648-17653.
34. Westlye LT, *et al.* (2010) Differentiating maturational and aging-related changes of the cerebral cortex by use of thickness and signal intensity. *Neuroimage* 52(1):172-185.
35. Westlye LT, *et al.* (2009) Increased sensitivity to effects of normal aging and Alzheimer's disease on cortical thickness by adjustment for local variability in gray/white contrast: a multi-sample MRI study. *Neuroimage* 47(4):1545-1557.
36. Seldon HL (2005) Does brain white matter growth expand the cortex like a balloon? Hypothesis and consequences. *Laterality* 10(1):81-95.
37. Kabaso D, Coskren PJ, Henry BI, Hof PR, & Wearne SL (2009) The electrotonic structure of pyramidal neurons contributing to prefrontal cortical circuits in macaque monkeys is significantly altered in aging. *Cereb Cortex* 19(10):2248-2268.

38. Salthouse TA (1996) The processing-speed theory of adult age differences in cognition. *Psychol Rev* 103(3):403-428.
39. Kail R (1991) Developmental change in speed of processing during childhood and adolescence. *Psychol Bull* 109(3):490-501.
40. Deary IJ, Penke L, & Johnson W (2010) The neuroscience of human intelligence differences. *Nat Rev Neurosci* 11(3):201-211.
41. Alexander-Bloch A, Giedd JN, & Bullmore E (2013) Imaging structural co-variance between human brain regions. *Nat Rev Neurosci* 14(5):322-336.
42. Crossley NA*, et al.* (2014) The hubs of the human connectome are generally implicated in the anatomy of brain disorders. *Brain* 137(Pt 8):2382-2395.
43. Huntenburg JM*, et al.* (2017) A Systematic Relationship Between Functional Connectivity and Intracortical Myelin in the Human Cerebral Cortex. *Cereb Cortex* 27(2):981-997.
44. Raz N*, et al.* (2004) Aging, sexual dimorphism, and hemispheric asymmetry of the cerebral cortex: replicability of regional differences in volume. *Neurobiol Aging* 25(3):377-396.
45. Shafto MA & Tyler LK (2014) Language in the aging brain: the network dynamics of cognitive decline and preservation. *Science* 346(6209):583-587.
46. Herve PY, Zago L, Petit L, Mazoyer B, & Tzourio-Mazoyer N (2013) Revisiting human hemispheric specialization with neuroimaging. *Trends Cogn Sci* 17(2):69-80.
47. Greve DN & Fischl B (2009) Accurate and robust brain image alignment using boundary-based registration. *Neuroimage* 48(1):63-72.
48. Wood SN (2006) *Generalized Additive Models: An Introduction with R* (CRC Press, Boca Raton, FL).
49. Fjell AM*, et al.* (2010) When does brain aging accelerate? Dangers of quadratic fits in cross-sectional studies. *Neuroimage* 50(4):1376-1383.
50. Vertes PE*, et al.* (2016) Gene transcription profiles associated with inter-modular hubs and connection distance in human functional magnetic resonance imaging networks. *Philos Trans R Soc Lond B Biol Sci* 371(1705).
51. Solari SV & Stoner R (2011) Cognitive consilience: primate non-primary neuroanatomical circuits underlying cognition. *Front Neuroanat* 5:65.
52. Triarhou LC (2007) The Economo-Koskinas atlas revisited: cytoarchitectonics and functional context. *Stereotact Funct Neurosurg* 85(5):195-203.
53. Blondel VD, Guillaume JL, Lambiotte R, & Lefebvre E (2008) Fast unfolding of communities in large networks. *J Stat Mech-Theory E*.
54. Sporns O & Betzel RF (2016) Modular Brain Networks. *Annu Rev Psychol* 67:613-640.
55. Shinn M*, et al.* (2017) Versatility of nodal affiliation to communities. *Sci Rep* 7(1):4273.
56. Hartigan JA & Hartigan P (1985) The dip test of unimodality. *The Annals of Statistics*:70-84.
57. Benjamini Y & Yekutieli D (2001) The control of the false discovery rate in multiple testing under dependency. *Annals of statistics*:1165-1188.